Journal of Applied Polymer Science

Fracture Phenomena in Micro- and Nano-Layered Polycarbonate/Poly(vinylidene fluoride-*co*-hexafluoropropylene) Films Under Electric Field for High Energy Density Capacitors

Zheng Zhou,[1] Matt Mackey,[1] Kezhen Yin,[1] Lei Zhu,[1] Donald Schuele,[2] Lionel Flandin,[3] Eric Baer[1]

[1]Department of Macromolecular Science and Engineering, Case Western Reserve University, Cleveland, Ohio 44106

[2]Department of Physics, Case Western Reserve University, Cleveland, Ohio 44106

[3]LEPMI, UMR 5279, CNRS, Universite´ de Savoie, F-73376 Le Bourget Du Lac Cedex, France

Current address for Zheng Zhou: Intel Corporation, 5000 W Chandler Blvd, Chandler, AZ, 85226

Corresponding author: Z. Zhou (E-mail: zheng1.zhou@intel.com)

ABSTRACT: The long-term dielectric lifetime properties of multilayered polycarbonate/poly(vinylidene fluoride-*co*-hexafluoropropylene) [PC/P(VDF-HFP)] films were measured as a function of the layer thickness. An optimum layer thickness of 160 nm was determined with the longest dielectric lifetime. The morphology of the damaged sites after dielectric breakdown was examined using scanning electron microscope. Acoustic emission detection system was coupled with the dielectric setup to correlate fracture events and dielectric breakdown to thereby elucidate the mechanisms of the enhancements in dielectric lifetime properties. Two types of acoustic signals were always observed during the breakdown process for multilayered films. The high-amplitude signals were attributed to the formation of breakdown pinholes caused by the primary discharge from top to bottom electrode. The subsequent low-amplitude signals were attributed to internal discharges that could further damage the film. The total number of acoustic hits, in particular, low-amplitude hits, increased with decreasing layer thickness, indicating more internal discharges occurred along the layered interface. It was concluded that the breakdown event initiated at a defect initiated "hotspot" formed because of internal pressure buildup. The film was punctured when the pressure buildup inside the film overcame the mechanical strength of the film. More number of PC layers and layer interfaces were desirable to slow down and divert the damage propagation through the film thickness direction. The crazes in P(VDF-HFP) can, however, easily propagate across PC layers with less than 160 nm layer thickness. © 2013 Wiley Periodicals, Inc. J. Appl. Polym. Sci. **2014**, *131*, 39877.

KEYWORDS: dielectricproperties; extrusion; polycarbonates; films; thermoplastics

Received 11 May 2013; accepted 16 August 2013

DOI: 10.1002/app.39877

INTRODUCTION

Microlayer coextrusion is a novel polymer-processing technique that can tailor readily available polymers into high value-added products for specific purposes. This technique enables fabrication of polymer films that contain up to thousands of alternating two or three polymeric layers with a continuous layer thickness down to 10 nm. The production of nanometer-scale polymer layers has been proven to be able to enhance dielectric,[1–3] optical,[4,5] mechanical,[6–8] and gas transport[9] properties.

Polymer films are becoming more and more important in a wide variety of applications ranging from dielectric, optical, and mechanical to gas transport applications. The broad applications are made possible because polymer films have excellent dielectric breakdown strength, high transparency, flexibility, and high barrier to gases and/or moisture. Polymer film capacitors play an important role in energy storage, power conditioning, noise suppression, and signal coupling applications.[10–13] Among these dielectric applications, energy storage/power conditioning application is becoming more and more essential, driven by the next generation electric vehicles, in which fast charging and discharging of a large amount of the energy is required. For these applications, certain dielectric properties are desired for polymer film dielectrics: high breakdown strength, long dielectric lifetime, low dielectric hysteresis, etc.

Recent studies on the layered polymer capacitor films have focused on dielectric properties, including dielectric lifetime,[3] breakdown strength,[1,2] and hysteresis.[14] Significant enhancements were observed for dielectric lifetime and breakdown strength, and hysteresis was reduced by decreasing poly(vinylidene fluoride)(PVDF) layer thickness. Wolak[15] and Mackey[2]

Table 1. PC/P(VDF-HFP) Multilayer Films Under Investigation

HFP layer thicknesses (nm)	5000	2500	1250	630	310	160	80	40	20
Number of layers	3	5	9	17	33	65	129	257	513

[a] All multilayer films have a composition of 50/50 and film thickness of 10 μm.

studied the fracture mechanisms of the layered polycarbonate/poly(vinylidene fluoride-CO-hexafluoro propylene)[PC/P(VDF-HFP)] under divergent field (needle-plane electrode configuration) conditions. However, little has been done on studying the fracture mechanisms under uniform field, which is more close to the actual use condition of capacitor films.

Previous studies[6–8] of layered PC/poly(styrene-co-acrylonitrile) (SAN) sheets demonstrated a significant amount of enhancement in mechanical toughness. Through fracture mechanisms study, it was concluded that the enhancement was attributed to the formation of shear bands in PC layers, which absorbed energy, blunted the tip of the crack in SAN layers, and stopped the crack propagation. Inspired by the previous fracture mechanisms study on mechanical enhancement in layered PC/SAN sheets, it was equally important and of great interest to study the fracture mechanisms of PC/P(VDF-HFP) layered films in the dielectric lifetime test. The dielectric fracture mechanism study would allow us to design high energy density capacitor films better. Acoustic emission detection technique, coupled with dielectric setup, was used to monitor acoustic emissions produced within PC/P(VDF-HFP) films during the dielectric fracture. The acoustic emission signals, in addition to fracture imaging data and electric current profile, were used to record time evolution of a breakdown event and probe the mechanisms during dielectric fracture. The main goal of this article was to study the effect of layer thickness on the breakdown/fracture mechanisms in PC/P(VDF-HFP) films. Another goal of this article was to systematically study the effect of layer thickness on the long-term dielectric lifetime of PC/P(VDF-HFP) films by varying the number of layers while maintaining a constant film thickness and composition and to determine the optimum layer thickness in terms of the dielectric lifetime. It was reported[2,3] that the 32- and 256-layer systems demonstrated an increase in both long-term dielectric lifetime and short-term dielectric breakdown strength relative to control and blend films; however, no optimization has been done on the effect of layered thickness on the dielectric properties of layered PC/P(VDF-HFP) films. In this article, the PC and P(VDF-HFP) layer thickness was systematically decreased from 5 μm to 20 nm by increasing the number of layers from 3 to 513, and the total film thickness and film composition remained essentially constant.

MATERIALS AND METHODS

Micro- and Nano-Layer Film Fabrication Using Multilayer Coextrusion Technology

An approach of "forced assembly" multilayer coextrusion[16] was used to produce alternately layered films of a P(VDF-HFP) (Kynar® 2500) and a bisphenol A polycarbonate (PC, Makrolon® 2207). The P(VDF-HFP) copolymer had a comonomer content of 19 wt % HFP content.

Multilayered films with 3, 5, 9, 17, 33, 65, 129, 257, and 513 layers were fabricated with a total film thickness of approximately 10 μm and a ratio of PC to P(VDF-HFP) of 50/50 vol./vol. Control films of PC and P(VDF-HFP) as well as a 50/50 blend were extruded with the same film thickness of 10 μm. Corresponding nominal layer thicknesses were calculated and shown in Table 1. One layer of PC with half of the nominal layer thickness was kept on each side of the layered films to maintain low surface resistivity.

PC was chosen based on its excellent dielectric breakdown strength, electronic resistivity, mechanical properties, combined with adequate adhesion with P(VDF-HFP). P(VDF-HFP) copolymer was chosen for its high dielectric constant (ε_r=11.2) and rheological compatibility with PC for coextrusion at 240°C. Sacrificial low-density polyethylene skin layers with a melt flow index of 5.0, which were removed prior to dielectric testing, were coextruded on both sides of the films to improve the film surface smoothness and handleability[17].

Long-Term Dielectric Lifetime Measurements

The long-term dielectric lifetime test [**Figure** 1(**a**)] was carried out with a stable high-voltage DC power supply, Fluke® 410B, which has an output voltage of 0 to ± 10,000 VDC, and an output stability of ± 0.02% per day after warm-up. The applied electric field was maintained at 320 kV/mm for all the tested samples. Four repetitions were performed on each sample. Samples for the dielectric lifetime tests were prepared by sputtering 20-nm-thick gold electrodes on both sides of the films (Figure 1(b). The plane—plane electrode configuration could probe a

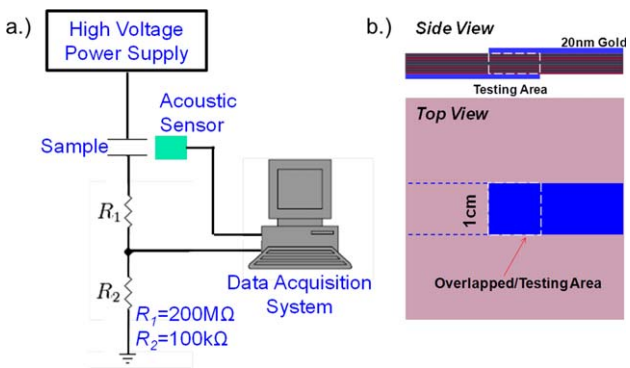

Figure 1. (a) A schematic showing the dielectric lifetime test and the acoustic emission setup for studying breakdown fracture mechanisms; (b) Sample preparation for studying breakdown fracture mechanisms. [Color figure can be viewed in the online issue, which is available at wileyonlinelibrary.com.]

large area in one experiment, which was equivalent to running many tests simultaneously. The testing area was 1 × 1 cm^2. The deposited gold electrodes ensured good electrical contact between the testing sample and the high-voltage power supply.

Electrical current versus time was determined during the lifetime test by measuring the voltage across a resistor using a data acquisition card (NI AT-MIO-16E-1). To keep voltages within the measurement range (±10 V), two resistors (200 MΩ and 100 kΩ) were used to form a voltage divider. The voltage across the precision 100 kΩ resistor was measured at a sampling rate of 100 Hz (Figure 1(a). The current profile was calculated from the voltage profile based on Ohm's law:

$$I(t) = \frac{V(t)}{R_2} \quad (1)$$

where R_2 is the precision 100 kΩ resistor, and $V(t)$ is the measured voltage across the resistor R_2 from the data acquisition card.

Acoustic Emission Detection of the Breakdown Event

An acoustic emission (AE) detection setup was incorporated with the dielectric lifetime setup to monitor AE signals during film breakdown. The sensor was purchased from Physical Acoustics Corporation (PAC®), a member of MISTRAS® Group Inc., with a resonant frequency at 150 kHz. Vacuum grease was used to ensure good attachment between the acoustic sensor and a polypropylene sheet on which the dielectric lifetime experiments were carried out. The layered film sample was placed on the polypropylene sheet and was positioned 10 cm away from the sensor. The AE signals were first preamplified at a fixed gain of 20 dB through a low-noise voltage preamplifier, PAC 2/4/6. The signals were then band pass filtered with a frequency range from 100 to 300 kHz. An acoustic amplitude threshold of 60 dB was chosen to remove all background noise. The acquisition and analysis of the signals were done using PCI/DSP-4P data acquisition card and AEwin® software, respectively.

Experimental Procedure to Observe Breakdown Cross Section of the Breakdown Event

After the layered film had a breakdown event, the fracture surfaces were examined under an optical microscope (OM). Features were best resolved in transmission mode using normal incidence illumination. The breakdown site of each sample was then sputtered with 10 nm of gold and examined in a JEOL JSM-6510LV scanning electron microscope (SEM) in secondary electron imaging mode.

The sample with the breakdown damage site was then embedded into epoxy resin and cured for at least 24. The sample in epoxy was polished to a desired wedge shape with a thickness down to 1 mm. Sand paper of 4000 grit was used to achieve high transparency across the film thickness direction. The wedges shape specimen was sliced using a Leica® EM UC 7 microtome at −50°C to get an ultra smooth cross section. The distance between the microtome knife tip and the breakdown hole can be measured using an OM under transmission mode as the epoxied sample was polished to be transparent. The specimen was cut to a desired distance from the central hole, removed from the microtome, and coated with 10 nm gold and examined in a JEOL JSM-6510LV SEM. An accelerating voltage of 30 kV and a working distance of 6 mm were chosen to achieve high magnification (>10,000×) images. High-magnification SEM images were taken quickly in order to prevent degradation of the samples. This process was repeated a few times to observe the cross sections at various distances from the central breakdown hole.

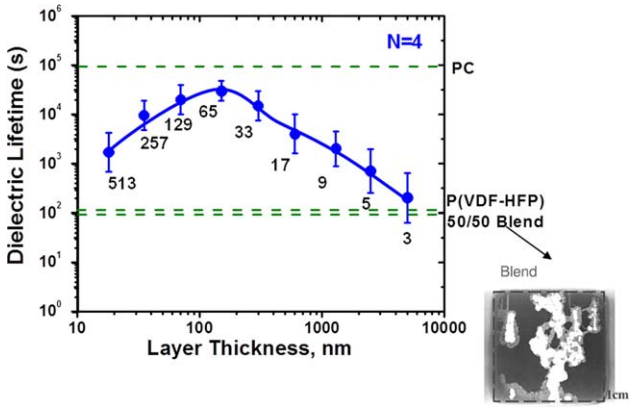

Figure 2. Dielectric lifetime as a function of layer thickness for PC/P(VDF-HFP) films with various number of layers. The PC, P(VDF-HFP), and 50/50 blend were also included and indicated as the dashed lines. The number next to the dots are the layer number of the film tested. The dielectric lifetime was obtained using a statistical analysis described in Ref. 3. The optical microscope image shows all damage holes on the 50/50 PC/P(VDF-HPF) blend film after dielectric lifetime test. [Color figure can be viewed in the online issue, which is available at wileyonlinelibrary.com.]

RESULTS AND DISCUSSION

Effect of Layer Thickness on the Dielectric Lifetime of Layered PC/P(VDF-HFP) Films

Figure 2 shows the dielectric lifetime of PC/P(VDF-HFP) multilayer films with various layer thicknesses. Values for PC and P(VDF-HFP) controls and 50/50 blend film were included for comparison. The ratio of PC to P(VDF-HFP) was 50/50, and the film thickness was maintained approximately 10 μm for both the layered and blend films. Accurate measurements of the thicknesses allowed applying a constant electric field of 320 kV/mm. The breakdown holes happen randomly. It can either be in the center of the film or along the edges/corners. An example of the breakdown evolution during dielectric lifetime test is shown in Ref. 3 (Figure 5). The detailed procedure describing the measurement of dielectric lifetime was reported in Ref. 3[3].

The 50/50 blend film exhibited the shortest dielectric lifetime of all tested films. It was even below both controls of individual polymers. The damage sites were shown in the inserted picture of Figure 2. On the structural standpoint, PC and P(VDF-HFP) are immiscible and physical blending induces phase separated domains. Thus, it appears that the interface between the two polymers is sensitive to the high electrical field and responsible for earlier failure of the blends. The reduction of lifetime may also partly result from the electric field enhancement caused by the large contrast in electrical properties of the two polymers. The breakdown holes of blend films were along elongated phase–separated domains, which were caused during extrusion process. In any case, the blending strategy is not desirable to improve the lifetime of polymers subjected to high electric field.

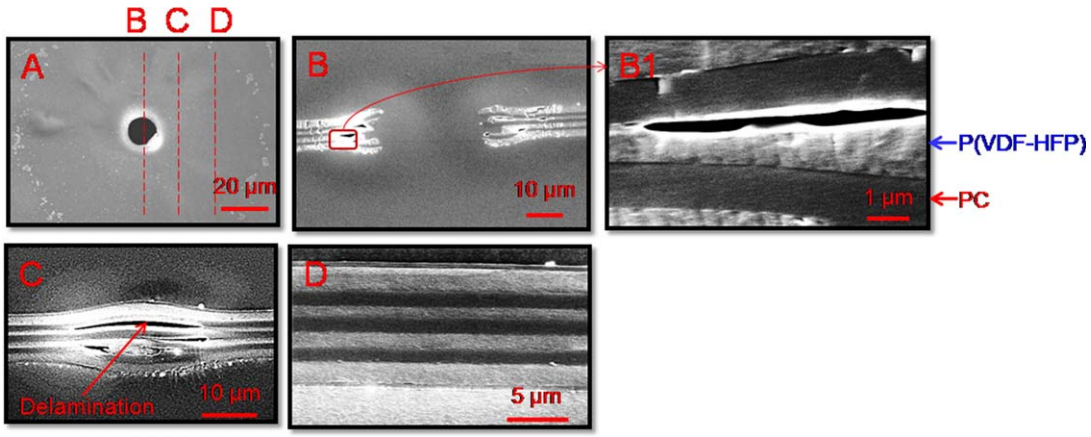

Figure 3. Cross-section images of the nine-layer PC/P(VDF-HFP) film after breakdown at various distances from the breakdown hole; (A) top view of the breakdown hole; (B) cross-section image right across the breakdown; (B′) zoom in image of B; (C) Cross section image: 25 μm from the breakdown hole; (D) cross-section image: 50 μm from the breakdown hole. The total film thickness is kept at 10 μm and the applied field is 320 MV/m. [Color figure can be viewed in the online issue, which is available at wileyonlinelibrary.com.]

In contrast, the dielectric lifetime increased substantially for PC/P(VDF-HFP) multilayer films, where the interfaces are arranged perpendicular to the electric field. As previously suggested,[2,15] the layered interfaces seem to delocalize the damage tip, prevent its propagation, and disfavor the breakdown across the film thickness. The lifetime varied from 200 to 30,000 seconds with decreasing the layer thickness from 5 μm to 160 nm. The 65-layer PC/P(VDF-HFP) film with a layer thickness of 160 nm exhibited the longest dielectric lifetime under the testing conditions.

For films with layer thickness thinner than 160 nm, the beneficial effect of layering two polymers, however, dropped gradually. A reasonable hypothesis to describe this limitation is related to the mechanical fracture damage that necessarily can propagate through the tough PC layers easily when the layers are too thin. Another hypothesis is that ultrathin PC layers fail to develop an electrical barrier effect. In other words, the charges trapped at the interfaces carry out internal discharges within thin PC layers. This means that electrons could tunnel through the glassy PC layers thinner than 160 nm under the applied electric fields. In order to further understand the major effect of layering on dielectric lifetime, the breakdown mechanisms during the dielectric lifetime test were investigated in more details through the observation of the damage areas.

The bulk PC film have longer dielectric lifetime than all layer 50/50 PC/P(VDF-HFP). In Ref. 2, the dielectric breakdown strength shows that PC control has lower dielectric breakdown strength than some of the 32-layer layered composites. The difference in the trend between the dielectric lifetime and breakdown strength measurements lies in the difference in the testing techniques. Reference 2 used need–plane electrode configuration. The dielectric lifetime test in this manuscript used plane–plane electrode.

SEM Imaging of 9-layer and 65-layer PC/P(VDF-HFP) Films under Constant DC Field of 320 MV/m

Figure 3 and Figure 4 are top-view and cross-section images of the multilayer films at several distances from the central breakdown hole for 9- and 65-layer films, respectively. Crazing, microcavitation, and delamination are evidenced on the B images. The cross-sectional images B and C gave some indications on nature of the breakdown event. Initially, high pressure built up in the central part of the layered film due to the vaporization of materials around the "hot spot".[18] When the internal pressure overwhelmed the mechanical strength of neighboring layers, the mechanical breakdown occurred, inducing microcavitation, delamination, and crazing in the film. The breakdown of the PC layer allowed the discharge of the charged species, simultaneously released the electric tension between layers.

Picture B′ is a zoom-in image of picture B in both Figure 3 and Figure 4. P(VDF-HFP) layers were brighter relative to PC under SEM because of its higher dielectric constant. Crazes with a width of around 400 nm were observed only in bright P(VDF-HFP) layers. PC layers remained intact. A smooth and featureless delamination tip was observed, indicating that the adhesion between PC and P(VDF-HFP) layers was overcome by the amount of energy released during breakdown.

The lateral delamination, which was also observed in the dielectric breakdown under divergent field,[2,15] deflected the propagation pathway and impeded the breakdown process, therefore, contributed to the enhanced dielectric lifetime. In addition, the textured nature of cross-section image B across the breakdown hole implied that crazing and dilation was also involved in the breakdown process to dissipate the input electric energy.

Effect of the Layer Thickness on SEM Cross-Section Images After Dielectric Breakdown

The cross-section images were taken for each sample with various layer thicknesses. It was first observed on the macroscopic scale that all breakdown damage zones extended approximately 50 μm from the center of the main breakdown hole. Figure 5 contains the representative images showing the effect of layer thickness on the breakdown fracture pattern across the breakdown hole under an electric field of 320 MV/m.

Three types of crazing were observed for all the tested samples. Crazes were not interconnected when the layer thickness was above 450 nm. The crazes were confined within a single

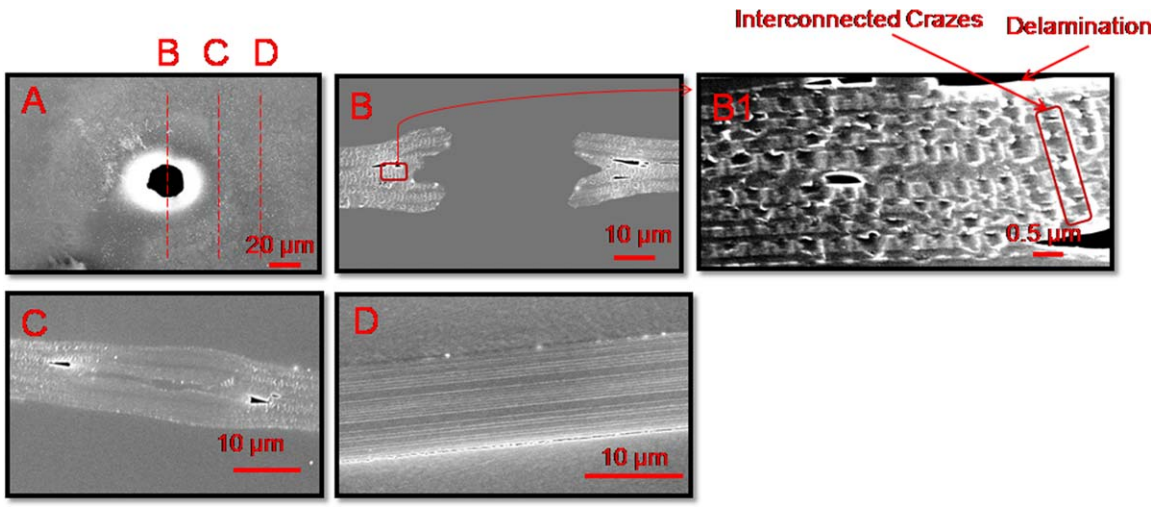

Figure 4. Cross-section images of the 65-layer PC/P(VDF-HFP) film after breakdown at various distances from the breakdown hole; (A) top view of the breakdown hole; (B) Cross-section image right across the breakdown; (B′) Zoom in image of B; (C) Cross section image: 25 μm from the breakdown hole; (D) Cross section image: 50 μm from the breakdown hole. The total film thickness is kept at 10 μm and the applied field is 320 MV/m. [Color figure can be viewed in the online issue, which is available at wileyonlinelibrary.com.]

P(VDF-HFP) layer. The height of the crazes was, therefore, the same as the layer thicknesses. The average width of the crazes was of around 400 nm. Additionally, stretched fibrils with a diameter close to 50 nm developed within those crazes (see the sketch in the images with layer thickness of 630 nm in Figure 5). In contrast, PC layers remained essentially intact. In addition to crazes, smooth delaminations with sharp tips occurred along the PC/P(VDF-HFP) interfaces, indicating weak interlayer adhesion.

When the layer thickness was in the range of 100 to 450 nm, parts of the crazes were interconnected across the film thickness direction. The craze density, defined as the number of crazes in a given area, increased drastically with decreasing layer thickness. The total amount of single crazes and craze arrays increased from 20 per 10 μm^2 for the film with PC layer thickness of 1.3 μm to 160 per 10 μm^2 for the film with PC layer thickness of 160 nm PC layers (Figure 6). The majority of the crazes were single crazes for all samples with layer thickness above 100 nm.

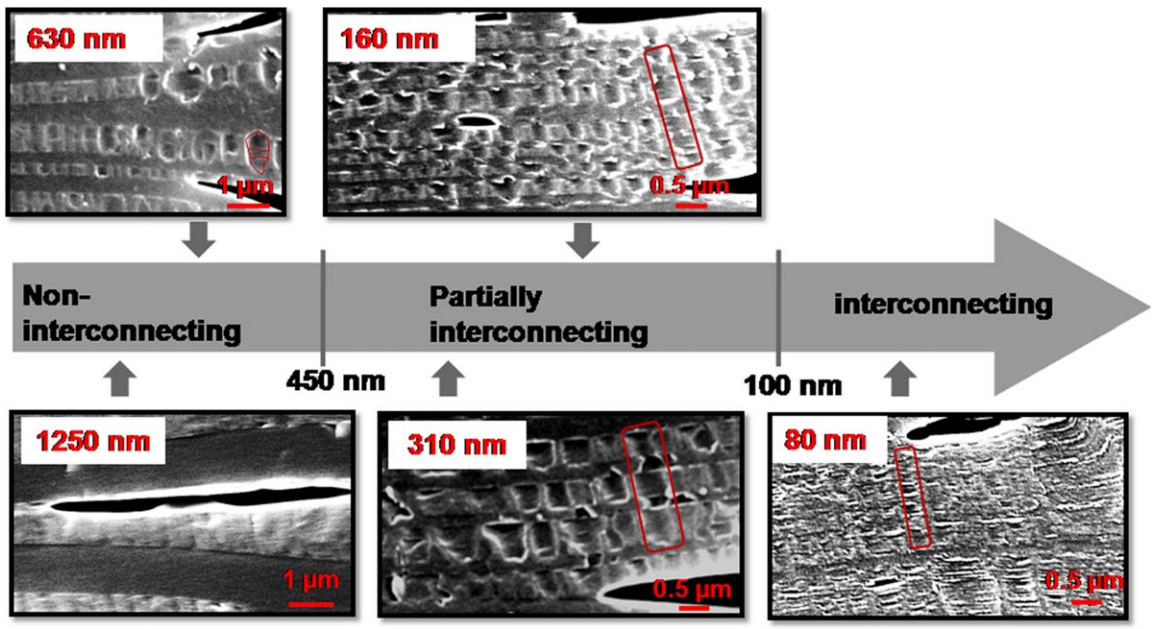

Figure 5. Representative images showing the effect of layer thickness on the type of crazing next to the breakdown hole after dielectric breakdown. Layer thickness for the samples are indicated on the top left corner of each image. The total film thickness is kept at 10 μm and the applied field is 320 MV/m. [Color figure can be viewed in the online issue, which is available at wileyonlinelibrary.com.]

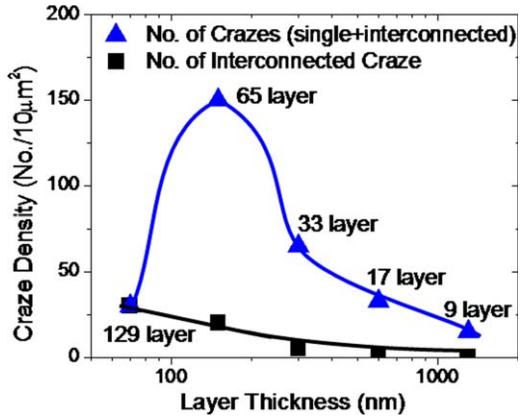

Figure 6. The craze density as a function of nominal tie layer thickness for PC/P(VDF-HFP) films with various number of layers. The total film thickness is kept at 10 μm and the applied field is 320 MV/m. [Color figure can be viewed in the online issue, which is available at wileyonlinelibrary.com.]

All crazes penetrated through many PC layers and interconnected with each other when the layer thickness decreased below 100 nm. The type of crazing in the film with 80 nm film was specific and qualitatively different from that observed with thicker PC layers. PC layers were so thin that the crazes propagated rapidly through many PC layers. An example of the craze arrays was indicated inside the rectangular box in the image with layer thickness of 80 nm in Figure 5.

To quantify the single craze and interconnected crazes, the craze densities and the percentage of interconnected crazes were counted and plotted as a function of PC layer thickness for the PC/P(VDF-HFP) films with various number of layers, Figure 6 and Figure 7(a). The total number of crazes including both single craze and interconnected crazes were counted in the images. The number of crazes gradually increased with the number of layers until the PC layer thickness reached 160 nm. For thinner PC layer, this amount dropped significantly because of a result of the development of the craze interconnectivity. In summary, Figure 5 follows a bell curve very similar in nature to that describing the dielectric lifetime in Figure 2. It is desirable to have more PC layers and interfaces to divert or delocalize the breakdown damages for the 10-μm-layered capacitor films. However, when the PC layers are too thin, the crazes can propagate rapidly through PC layers. These craze arrays indicate thinner PC layers are not as effective as thicker PC layers in terms of slowing down or stopping the craze propagation. This could explain the existence of an optimum thickness of 160 nm for achieving the longest dielectric lifetime.

Similar phenomenon described as "interactive crazing" was observed in mechanical tensile test of PC/SAN layered sheet, Figure 7(**b**).[6,7] Similarly, three types of crazing: single crazes, partially craze arrays, and craze arrays were observed as a function of PC layer thickness. The transition region, partially craze arrays region, had a PC thickness of 1.3 to 6 μm during mechanical tensile test. The transition region, partially craze arrays region, for dielectric lifetime test had a PC thickness of 100 nm to 450 nm. The difference in the transition PC layer thickness was from the difference in testing conditions, specifically testing frequency.

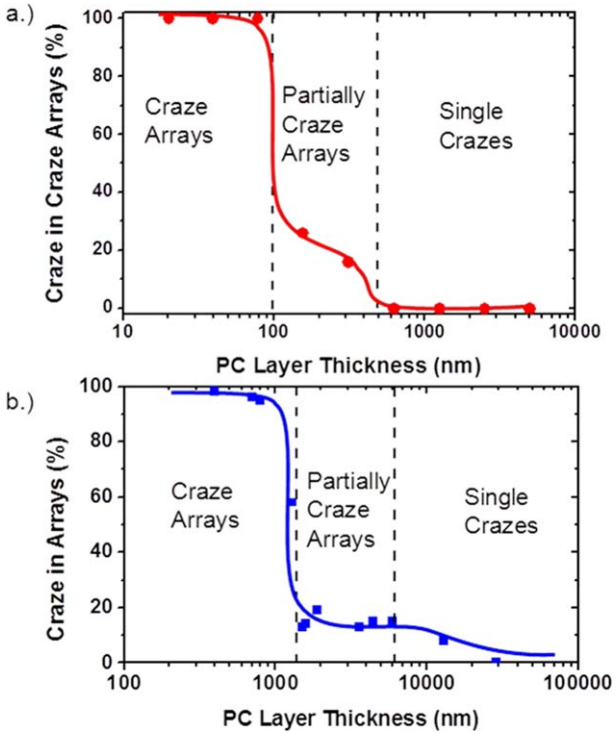

Figure 7. (a) Types of crazing as a function of PC layer thicknesses for PC/P(VDF-HFP) films with various number of layers for dielectric test. The total film thickness is kept at 10 μm and the applied field is 320 MV/m. (b) Types of crazing as a function of PC layer thicknesses for PC/SAN sheets with various number of layers for mechanical tensile test. The data were from D. Haderski, et al[6]. [Color figure can be viewed in the online issue, which is available at wileyonlinelibrary.com.]

During the dielectric lifetime test, film discharge breakdown event had a time duration of micron-seconds or breakdown frequency of approximately 10^6 Hz, and the testing frequency of conventional mechanical tensile test was approximately 1 Hz. It is also shown that the crazes tend not to connect when increasing testing speed or frequency.[6] In addition, the damage zones tend to become smaller when increasing testing frequency during fatigue testing of a polymeric sample.[19,20] The glass transition temperature shifts to higher temperature and the material becomes harder with increasing testing frequency. The PC tested at 10^6 Hz is stronger and harder for crazes to penetrate through. All of the above statements could explain that the layer thickness for the transitional region was smaller for dielectric test, which had a higher testing frequency.

Acoustic Emission Signals and Electric Current Profile of 65-Layered PC/P(VDF-HFP) Films Under Constant DC Field of 320 MV/m

Acoustic emission technique was incorporated with dielectric lifetime setup to monitor acoustic emission signals emitted from PC/P(VDF-HFP) films during dielectric fracture process. The layered films were stressed under a DC field of 320 kV/mm until a breakdown event occurred. A threshold of 60 dB was chosen to eliminate the background noise.

Under these conditions, no current spikes or acoustic hits were detected until film breakdowns happened. For each breakdown

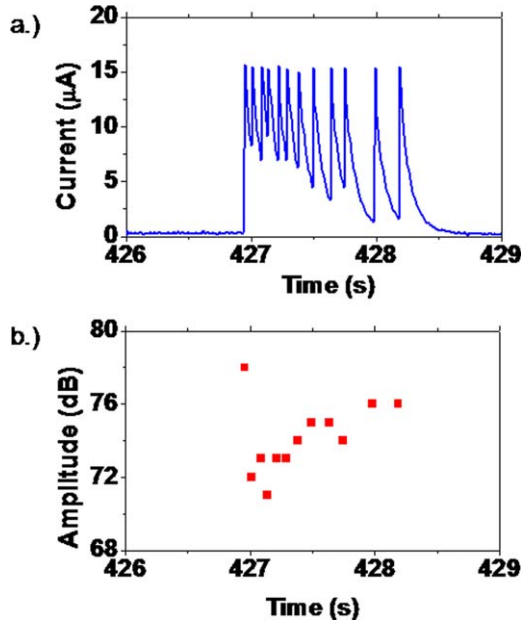

Figure 8. (a) Electric current profile and (b) acoustic amplitude data for the breakdown event of the 65-layer 50/50 PC/P(VDF-HFP) film; The total film thickness is kept at 10 μm and the applied field is 320 MV/m. [Color figure can be viewed in the online issue, which is available at wileyonlinelibrary.com.]

event, a series of current peaks and acoustic hits were observed for all samples. For all the observed events, a current peak corresponded to an acoustic hit. The monolithic control films qualitatively differed from the layered films in the acoustic amplitude profile. For the controls, all acoustic amplitudes were similar and relatively high (above 75 dB). If the layered films also exhibited a high initial acoustic amplitude (above 75dB), the subsequent acoustic amplitude always was significantly lower (~65 dB). The third and subsequent events increased again to high amplitude (above 75 dB) (Figure 7).

The energy charged into the capacitor films is expressed based on equation

$$E_c = \frac{1}{2}CV^2 = \frac{1}{2}\frac{Q^2}{C} \quad (2)$$

$$lgE_c = 2lgQ - \lg(2C) \quad (3)$$

where E_c is the energy charged into the capacitor film, C is the film capacitance, V is the voltage across the resistor, and Q is the charge input into the capacitor film. Assuming that C remains constant before and after the breakdown event, lgQ has a linear relationship with lgE_c. The acoustic amplitude can be expressed as equation

$$A = 10lg\frac{E_a}{E_{ref}} \quad (4)$$

$$A = 10lgE_a - 10lgE_{ref} \quad (5)$$

where A is the acoustic amplitude, E_a is the acoustic energy, and E_{ref} is the reference energy and equals 10^{-12} J/m^3 Therefore, acoustic amplitude A has a linear relationship with lgE_a.

The input charge calculated from the integration of the current peak and acoustic amplitude was plotted (Figure 9). The logarithmic charge calculated from the area under the current profile increased linearly with acoustic amplitude for layered PC/P(VDF-HFP) films, which indicated that lgQ has a linear relationship with A. lgQ had a linear relationship with lgE_c and A has a linear relationship with lgE_a; therefore, lgE_c and lgE_a were linearly related. The linear relationship indicated the acoustic signals were intercorrelated with electric signals for all acoustic hits.

For monolithic PC and P(VDF-HFP) controls, all acoustic amplitude signals were above 75 dB (solid rectangles and circles in Figure 9). The different trends for controls and layered PC/P(VDF-HFP) films in amplitude versus. logarithmic charge gave us indirect proof that the breakdown mechanisms were different for controls and layered films. It is proposed that the initial high amplitude acoustic emission was from the discharge from the top to the bottom electrode, and subsequent low amplitude acoustic emissions were from internal discharges along the layer interfaces. The controls only exhibited high amplitude signals because there was no discharge along the layered interfaces.

Figure 10 shows the effect of the layer thickness on the number of acoustic hits during a breakdown event of layered PC/P(VDF-HFP) films. The number of acoustic hits for PC and P(VDF-HFP) monolithic controls was shown as arrows on the right side of the plot. The total number of acoustic hits, mainly the low amplitude acoustic hits produced by the discharge along the layered interfaces, increased gradually with decreasing the layer thickness. In other words, the discharge along the layered interfaces happened more easily within films with thinner layers.

Proposed Breakdown Mechanism Based on the Fracture Images, Acoustic Signals, and Electrical Current Profile

Currently, there is no explicit model that can explain the lifetime data seen in multilayered films with various layer thicknesses (Figure 2). However, based on the fracture images, acoustic signals and electrical current profile, a breakdown

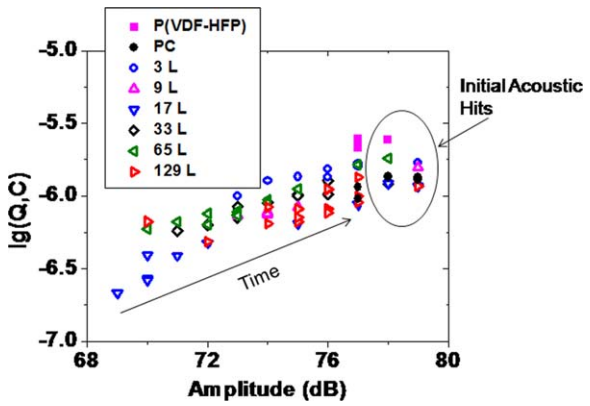

Figure 9. Correlation between the acoustic amplitude and the input charge obtained from current profile in the 50/50 PC/P(VDF-HFP) system with various number of layers. The total film thickness is kept at 10 μm and the applied field is 320 MV/m. [Color figure can be viewed in the online issue, which is available at wileyonlinelibrary.com.]

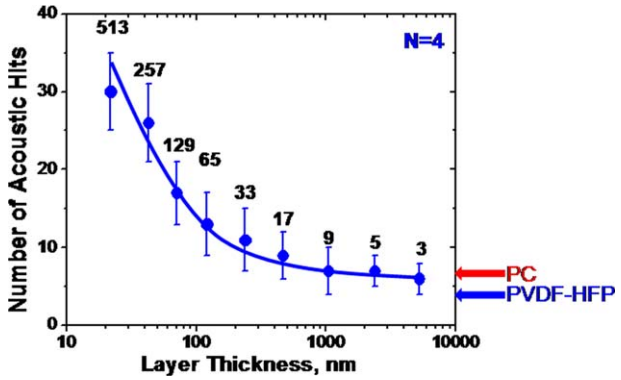

Figure 10. Effect of layer thickness on the number of acoustic hits during a breakdown event of PC/P(VDF-HFP). The numbers next to the dots are the layer number of the film tested. The total film thickness is kept at around 10 μm and the applied field is 320 MV/m. [Color figure can be viewed in the online issue, which is available at wileyonlinelibrary.com.]

mechanism during the dielectric lifetime test is proposed (Figure 11).

After applying electric field for some time, a "hot spot" forms along a conductive pathway.[18] High pressure builds up inside the layered film due to the vaporization of materials around the "hot spot". The film is punctured when the pressure buildup at the hot spot overcome the mechanical strength of layered films. Main breakdown hole forms, and the film discharges. Crazing, microcavitation, and delamination happen during the puncture of the film, inducing the loudest acoustic hit. The subsequent acoustic hits, with lower amplitudes, happen because of internal discharge along the layered interfaces. These hits further damage the film and evaporate the electrodes. The breakdown events are interrupted and the conductive pathway inside the capacitor film formed previously is decomposed in this series of rapid occurring events. In such a way, catastrophic damage and failure of the capacitor are prevented. As long as the PC layers remain tough enough to mechanically hold the structure, the lifetime is enhanced by the increase of amount of interface. For very large number of layers, however, the barrier effect is partially lost because of the lack of strength of thin PC layers. In summary, an optimum layer thickness of about 160 nm is observed corresponding to the longest dielectric lifetime.

CONCLUSIONS

The forced assembly approach of microlayering lead to alternate layers of polymers with enhanced dielectric lifetime properties. The lifetime increased from 200 to 30,000 s by increasing the number of layers within the films from 3 to 65. An optimum layer thickness of 160 nm was found for achieving the longest dielectric lifetime.

Dielectric fracture image analysis revealed that the damages were delocalized by the blocking electrode PC layers and the interfaces. Three types of crazing were observed in P(VDF-HFP) layers for PC/P(VDF-HFP) systems with a wide range of layer thicknesses. The crazes were noninterconnecting and confined in only one P(VDF-HFP) when the PC layer thickness was above 450 nm. Those crazes started to interconnect when the layer thickness decreased. A partially craze arrays region was found in between 450 and 100 nm. When the layer thickness was further reduced to down below 100 nm, crazes could penetrate PC layers and interconnect with each other. The total number of crazes also followed a bell curve as a function of the PC layer thickness. The two properties (lifetime and number of crazes) were closely interrelated with maxima at about 160 nm.

A similar phenomenon on the types of crazing was observed in the mechanical tensile test of PC/SAN layered sheets. A difference was observed in the layer thickness of the transition region from single craze to partial craze arrays. The PC layer thickness of the transition region for tensile test was 1.3 to 6 μm, and the PC layer thickness of the transition region for dielectric test was 100 to 45 nm. The difference in the PC layer thickness lies in the testing frequency. High frequency testing disfavors the interconnection between the crazes shifting the transition to lower thicknesses.

The acoustic signals indicated that the high-amplitude signals were from the main breakdown hole formation caused by the pressure buildup inside the film. The subsequent smaller

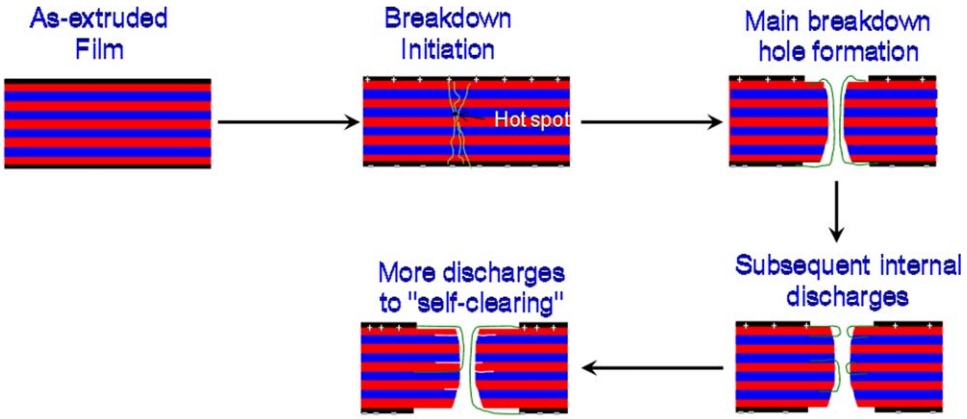

Figure 11. Schematic representation of the time evolution of a breakdown event. Black, red, and blue colors represents electrodes, PC layers, and P(VDF-HFP) layers, respectively. Solid green lines are electric current. [Color figure can be viewed in the online issue, which is available at wileyonlinelibrary.com.]

amplitude signals were from the internal discharges along the layered interfaces. The film with thinner layers discharged along the layered interfaces more easily because of smaller interlayer distances, which was not desirable for capacitor applications.

A breakdown mechanism for the dielectric lifetime measurement is proposed based on the data presented to explain the optimum layer thickness observed in the dielectric lifetime data. PC layers, in additional to the multiple layer interfaces, acted as barrier layers to slow down or divert damage propagation through the film thickness direction, thus prolonging the lifetime. However, if the PC layers were too thin, the crazes formed in P(VDF-HFP) layers can penetrate rapidly through the PC layers and the damage can propagate rapidly across the film. In addition, the film discharge happened more easily when the thickness of PC layers was thin, which was also not desirable for energy-storage applications.

ACKNOWLEDGMENTS

This research was generously supported by the National Science Foundation through the Center for Layered Polymeric Systems (CLiPS) Science and Technology Center, grant DMR-0425914 and the Office of Naval Research grant N00014-11-0215.

REFERENCES

1. Wolak, M. A.; Pan, M. J.; Wan, A.; Shirk, J. S.; Mackey, M.; Hiltner, A.; Baer, E.; Flandin, L. *Appl. Phys. Lett.* **2008**, *92*, 113301.
2. Mackey, M.; Hiltner, A.; Baer, E.; Flandin, L.; Wolak, M. A.; Shirk, J. S. *J. Phys. D: Appl. Phys.* **2009**, *42*, 175304.
3. Zhou, Z.; Mackey, M.; Carr, J.; Zhu, L.; Flandin, L.; Baer, E.; *J. Polym. Sci. Part B: Poly. Phys.* **2012**, *50*, 14, 993.
4. Ji, S.; Ponting, M.; Lepkowicz, R.; Rosenberg, A.; Flynn, R.; Beadie, G.; Baer, E. *Optics Express* **2012**, *20*, 26746.
5. Armstrong, S.; Zhou, Z.; Hiltner, A.; Baer, A. *J. Appl. Polym. Sci.* **2009**, *113*, 2150.
6. Haderski, D.; Sung, K.; I, J.; Hiltner, A.; Baer, E. *J. Appl. Polym. Sci.* **1994**, *52*, 121.
7. Sung, K.; Haderski, D.; Hiltner, A.; Baer, E. *J. Appl. Polym. Sci.* **1994**, *52*, 147.
8. Sung, K., Hiltner, A., Baer, E. *J. Mater. Sci.* **1994**, *29*, 5559.
9. Wang, H.; Keum, J.; Hiltner, A.; Baer, E.; Freeman, B.; Rozanski, A.; Galeski A. *Science* **2009**, *323*, 757.
10. Mackevich, J.; Shah, M. *IEEE Electr. Insul.* **2002**, *13*, 5.
11. Mackevich, J.; Simmons, S. *IEEE Electr. Insul.* **2002**, *13*, 10.
12. Clelland, I.; Price, R. Proc. 8th Ann. Eur. Capacit. Resist. Tech. Symp., Manchester, UK **1994**.
13. Jain, P.; Rymaszewski, E. Thin Film Capacitors for Packaged Electronics, Kluwer: Norwell, MA, **2004**.
14. Mackey, M.; Schuele, D.; Zhu, L.; Baer, E. *J. Appl. Phys.* **2012**, *111*, 113702.
15. Wolak, M.; Wan, A.; Shirk, J.; Mackey, M.; Hiltner, A.; Baer E. *J. Appl. Polym. Sci.* **2012**, *123*, 2548.
16. Mueller, C.; Kerns, J.; Ebeling, T.; Nazarenko, S.; Hiltner, A.; Baer, E. In: Polymer Processing Engineering, Coats, R., Eds.; Institute of Materials: UK, **1997**.
17. Kazmierczak, T.; Song, H.; Hiltner, A.; Baer, E. *Macromol. Rapid Commun.* **2007**, *28*, 2210.
18. Reed, C.; Cichanowski, S. *IEEE Trans. Dielectr. Electr. Insul.* **1994**, *1*, 904.
19. Parsons, M.; Stepanov, E.; Hiltner, A.; Baer, E. *J. Mater. Sci.* **2000**, *35*, 1857.
20. Zhou, Z.; Hiltner, A.; Baer, E. *J. Mater. Sci.* **2011**, *46*, 174.